Received 22 February 2009
Revised 14 April 2009
Accepted 20 April 2009

The effect of up-armoring of the high-mobility multi-purpose wheeled vehicle (HMMWV) on the off-road vehicle performance

M. Grujicic, H. Marvi, G. Arakere, W.C. Bell and I. Haque
Department of Mechanical Engineering,
International Center for Automotive Research CU-ICAR,
Clemson University, Clemson, South Carolina, USA

Abstract

Purpose – A parallel finite-element/multi-body-dynamics investigation is carried out of the effect of up-armoring on the off-road performance of a prototypical high-mobility multipurpose-wheeled vehicle (HMMWV). The paper seeks to investigate the up-armoring effect on the vehicle performance under the following off-road maneuvers: straight-line flatland braking; straight-line off-angle downhill braking; and sharp left turn.

Design/methodology/approach – For each of the above-mentioned maneuvers, the appropriate vehicle-performance criteria are identified and the parameters used to quantify these criteria are defined and assessed. The ability of a computationally efficient multi-body dynamics approach when combined with a detailed model for tire/soil interactions to yield results qualitatively and quantitatively consistent with their computational counterparts obtained using computationally quite costly finite element analyses is assessed.

Findings – The computational results obtained clearly reveal the compromises in vehicle off-road performance caused by the up-armoring employ to improve vehicle blast and ballistic protection performance/survivability. The results obtained are also analyzed and explained in terms of general field-test observations in order to judge physical soundness and fidelity of the present computational approaches.

Originality/value – The paper offers insights into the effects of up-armoring of the HMMWV on off-road vehicle performance.

Keywords Road vehicles, Finite element analysis, Modelling, Simulation

Paper type Research paper

1. Introduction

In the late 1970s, the US Army identified a need for a better-performing light tactical vehicle to replace a number of vehicles then in use (e.g. the M561 Gama Goat, the M151-series Jeeps, and civilian trucks adapted for military use) which had proved not

The material presented in this paper is based on the work supported by a research contract with the Automotive Research Center at the University of Michigan and TARDEC. The authors are indebted to Professor Georges Fadel for the support and a continuing interest in the present paper.

Multidiscipline Modeling in Materials and Structures
Vol. 6 No. 2, 2010
pp. 229-256

1573-6105
DOI 10.1108/15736101011068019

very reliable, to have problems related to payload limitations and safety characteristics and to fall short in meeting the military mission requirements, in general. That is how the concept for the high-mobility multi-purpose wheeled vehicle (HMMWV) family of vehicles was born. The main characteristics of the HMMWV family were identified as:

- highly versatile;
- technologically advanced;
- cross-country ready;
- capable of performing both combat and combat-support roles;
- based on a basic chassis capable of being modified into a number of variants;
- diesel-powered in order to be consistent with the Army's desire to use diesel fuel throughout its tactical vehicle fleet; and
- equipped with an automatic transmission.

Recently, virtually all of the US military branches use the HMMWV as the standard utility vehicle for logistical support and convoy operations. There are also exceptions to this traditional application of the HMMWV, such as its use in Cavalry and Infantry Scout units where this vehicle is utilized in offensive and defensive missions and where, in order for the HMMWV to fulfill functional requirements of these missions, it is usually fully or partially up-armored. However, the tactical and operational environments of Operation Iraqi Freedom and Operation Enduring Freedom have resulted in a major role change for the HMMWV. That is, as clearly evidenced in these operations, enemy contact is no longer defined as a discernable front line that can be physically identified on a map. Instead, the battle-field can be more-accurately described as being non-linear and asymmetrical and, consequently, units are forced to operate in zones that are susceptible to enemy contact from any direction at any time. This means that supply lines and logistical missions that were historically secure now operate in potentially hostile areas and are always vulnerable to attack (Stewart, 2006; Law *et al.*, 1998). Hence, the majority of (non-armored) HMMWVs are now operating in conditions for which they were not originally designed and are subjected to harsh maneuvers that they would not traditionally have to conduct. This situation has resulted in a significant increase in rollover and instability-related HMMWV accidents during such highly dynamic maneuvers and, in turn, to an increase in soldier injuries and fatalities.

The aforementioned situation has been made even worse by retrofit up-armoring of the HMMWVs. That is, in order to address the problems associated with road landmines and improvised explosive devices (IEDs), units have responded with force protection measures involving up-armoring of all HMMWVs (either by contractors, using retro-fit add-on armor kits or armor internally fabricated from steel, sand-bags, etc.). While the additional armor has increased vehicle blast/ballistic protection performance, it has also degraded its riding-stability performance because suspension and steering components and tires have not been modified (in most cases) to keep pace with the added weight of installed armor (the mass of additional armor can be up to 2,000 kg). This has further contributed to the increase in HMMWV instability-related accidents and soldier injuries/fatalities. In addition, frequent accidents have also occurred when, due to excessive weight of the up-armored

HMMWV, the roadside or a small bridge would collapse causing the vehicle to land in the ditch/water and soldier injuries/fatalities.

A photograph of the HMMWV M1025 is shown in Plate 1. The HMMWV model analyzed in the present work mimics the M1025. However, it should be noted that limited effort was made to closely match the key geometrical, kinematic and compliance parameters of the M1025. This was done so intentionally for the following two reasons:

(1) to prevent the potential misuse of the results obtained in the present work; and

(2) the main effort in the present work was to reveal the general compromising effects of up-armoring on the vehicle off-road performance.

As discussed earlier, as the existing HMMWVs are being up-armored to enhance their blast/ballistic-protection performance and survivability, the driving performance, stability and safety of these vehicles (particularly during off-road travel) are being seriously compromised, due to extra weight associated with the added armor. This loss in performance means that the up-armored HMMWV is less than ideal for some of the missions it was originally intended for. In our recent work (Grujicic *et al.*, 2008a), a series of preliminary finite element computational analyses of several HMMWV maneuvers on a sandy road were carried out in order to assess the effect of vehicle up-armoring on its off-road performance. The results obtained not only showed the undesirable effects of vehicle up-armoring, but also clearly revealed a very high-computational cost associated with the use of the finite element analysis.

Traditionally, computational investigations of the vehicle performance are based on the use of multi-body vehicle-dynamics analyses (Hahn *et al.*, 2007). In these investigations, special force elements are used to account for the interaction between the tires and the road. While multi-body computational analyses are very efficient, i.e. associated with a low-computational cost, their results are highly dependent on the functional forms and parameterization of the force elements (Lee and Kiu, 2007).

Plate 1.
Photograph of a HMMWV M1025, the vehicle analyzed in the present work

In the case of off-road vehicle performance analysis, the availability of high-fidelity robust models for the tire/soil interaction force elements is particularly critical. In our recent work (Grujicic *et al.*, 2008a, b, 2009, 2010), finite element simulations of tire/sand interactions under different conditions of inflation pressure, vertical load, friction coefficient, longitudinal slip, and slip angle were used to formulate and parameterize a tire/soil interaction force element for the case of the Goodyear Wrangler HT LT 235/H5 R15 tire and prototypical dry sand. Limited experimental data were then used to validate the model.

The main objective of the present work is to carry out a series of parallel finite-element/multi-body-dynamics simulations of several HMMWV maneuvers in order to:

- assess vehicle's off-road performance; and
- determine the ability of the computationally very efficient multi-body vehicle dynamics analysis (based on the use of the detailed tire/soil force-elements model (Grujicic *et al.*, 2008a, b, 2009, 2010)) to accurately predict this performance.

Design of vehicles for off-road performance relies typically on the extensive use of experimental test and development programs. While the use of these experimental programs is highly critical, they are generally expensive and time-consuming. Consequently, experimental testing programs are gradually being complemented by computational engineering analyses and simulations. In recent years, major advances have been made in modeling entire vehicles and their performance under various standard driving and extreme maneuvering conditions (Grujicic *et al.*, 2007, 2008b), the constituent response of the materials under high deformation-rate, large-deformation conditions, and the interactions between deformable solids and between fluids and solids (Grujicic *et al.*, 2007, 2008b). In particular, these models have enabled the coupling between Eulerian representations (typically applied to the gaseous and liquid domains) and Lagrange representations (typically applied to solid domains). These advances in the computational modeling and simulations combined with the major advances in the computational software and hardware are gradually enhancing the fidelity of the computational engineering analyses to the level that, in the near future, virtual design, development and validation of complete vehicles, and their sub-systems may become reality. Hence, one of the main objectives of the present paper is to help with a further development of these computational engineering analyses and simulations so that they can become a reliable method/alternative in the development process of high off-road performance vehicles.

The organization of the paper is as follows: a brief description of the problem definition, geometrical models for the vehicle and a sandy road, the associated material models and details of the computational procedure used in the finite element-based transient non-linear dynamics analysis of the off-road vehicle performance are all presented in Section 2.1. The problem definition, topology of the vehicle model and details of the computational procedure used in the multi-body dynamics (MBDs) analysis, including the tire/sand mode of the same off-road vehicle performance are all presented in Section 2.2. The results obtained in the present work are presented and discussed in Section 3. The main conclusions resulting from the present work are summarized in Section 4.

2. Modeling and computational procedures

2.1 Finite element modeling and simulations of the off-road HMMWV maneuvers

In this section, a brief description is given of the computational analyses used to model the behavior of a HMMWV (in a standard configuration and in an up-armored configuration) during three off-road maneuvers:

(1) straight-line flatland braking;

(2) straight-line off-angle downhill braking (i.e. braking during downhill travel of the vehicle in a direction which makes an angle with the straight-downhill direction); and

(3) sharp left turn.

The computational modeling of this behavior involves two distinct steps:

(1) geometric modeling of the two configurations of the HMMWV and sand-bed; and

(2) the associated transient non-linear dynamics analysis of the vehicle off-road maneuvers.

Since both of these steps were presented in great details in Grujicic *et al.* (2008a), only a brief overview of each will be presented here. All the calculations carried out in this portion of the work were done using ABAQUS/Explicit, a general-purpose transient non-linear dynamics analysis software (Dassault Systems, 2008). In our previous work (Grujicic *et al.*, 2008a), a detailed account was provided of the basic features of ABAQUS/Explicit, emphasizing the ones which are most relevant for modeling vehicle off-road performance.

2.1.1 Geometric model for the HMMWV. The finite element model of the HMMWV (with an overall length of 4.84 m and a wheelbase of 3.4 m) used in the present work consists of approximately 150,000 elements. The CAD model originally developed by D. Wilson was purchased from 3DCAD.com (CAD Browser, 2010) and preprocessed for ABAQUS/Explicit finite element program (Dassault Systems, 2008) using the general purpose pre-processing program HyperMesh from Altair, Inc. (Altair Engineering, 2010). The model includes the following subsystems: chassis, front and rear suspension, four wheels, steering, engine, transmission, cabin, hood, and four doors and four seats. Each sub-system, in turn, consists of a number of parts/components. A summary of the main parts which were included in the HMMWV finite element model can be found in Table I.

The parts are meshed with three-dimensional shell elements, three-dimensional beam elements, and three-dimensional solid elements and assembled by either using various connector elements, tying their adjacent edges/faces or by having the connected parts share their edge nodes. Engine block, brake assemblies, front and rear differentials, transfer case, and chassis frame rear axel are modeled as rigid parts in order to take advantage of the high stiffness of these parts relative to other parts. Independent front and rear suspension systems are each modeled using a parallel spring/damper arrangement. Each of the four wheel rims were connected to their respective wheel hub using a combination of Cartesian and Cardan connectors and subjected to the appropriate surface-to-node kinematic coupling constraints. This enables independent prescription of the wheels rotational and steering velocities.

Part name	No. of parts	Part description/function
Tires, wheel, and braking		
Tires	4	Provide traction with the road
Rims	4	Connect the tire to the brake assembly
Brake discs	4	A simple model of the brake disc
Wheel hubs	4	Connect the wheel to the steering assembly
Suspension		
Upper A-arms	4	Allow for vertical motion of wheels
Lower A-arms	4	Allow for vertical motion of wheels and shock mount
Spring/shock absorbers	4	Absorb shock and dampens vibrations
Shock absorber mounts	4	Support the damper/shock absorber
Cross members	4	Connect the lower A-arms
Steering		
Steering system	1	Allows driver to control the vehicle
Chassis		
Main frame	1	Provides longitudinal bending/torsional stiffness
Cross members	2	Provide transverse connection in the main frame
Engine and transmission		
Engine	1	Provides the power to the vehicle
Differential	2	Supplies torque independently to the wheels
Transfer case	1	Transmits input transmission power to the front and rear wheels
Engine gearbox	1	Engine gearing and transfer of power to drive shaft
Drive shaft	3	Drives the train members
Front and rear axles	2	Transmit power to the wheels
Body		
Cabin floor	1	A simple model of the driver compartment
Roof/roof closure	1	A simple model of a roof/roof closure
Interior panel	2	Provides support to the driver compartment
Windshield/window	6	A simple model of the windshield/window
Doors	4	A simple model of the cabin door
Hood	1	Provides upper closure to the engine compartment
Seat	4	Interior driver and passenger seating

Table I.
Names and descriptions of the parts used in the finite element analysis of the HMMWV M1025

Two configurations of the HMMWV:

(1) a standard configuration; and

(2) an up-armored configuration are considered in the present work.

While most HMMWV models are not required by the US military to have any armor protection, armament carriers and the hard-shelled ambulance models were designed to provide some minor level of protection. The "basic" armor package used is a combination of steel, Kevlar®-reinforced composites, and laminated glass/ polycarbonate windshield/windows designed to stop a fragment weighing less than 1.5 g. The "supplemental" armor provides an additional level of protection to stop fragments weighing less than 4 g. The standard HMMWV configuration used in the present work was equipped with the basic armor package. Clearly, neither basic nor supplemental armor is capable of defeating commonly encountered bullets at full muzzle velocity or average-size IED fragments. Hence, the up-armored configuration of the HMMWV was also considered in this work. In this configuration, additional steel and Kevlar®-reinforced composite armor panels were applied to the vehicles underbody and doors, and larger gauge laminated transparent-armor panels were used for the windshield and windows. The gross weight of the up-armored HMMWV configuration was ca. 1,500 kg greater than that of the standard configuration. Owing to the sensitive nature of the subject matter and the potential for misuse of the up-armored vehicle model, no further details could be provided here.

The standard SAE coordinate system was used, i.e. the finite element model of the HMMWV, Figure 1, is oriented in such a way that the positive x-direction goes from the rear to the front of the vehicle, the positive y-direction goes from the passenger (right-hand) side to the driver (left-hand) side, and the positive z-direction is upward.

The materials used in the HMMWV model are idealized as rigid (used only in some beam connectors, brakes, and brake assemblies), linear elastic, hyper-elastic, elastic-plastic or elastic-plastic with failure. Suitable adjustments are made to the material properties in order to account for non-modeled features of various parts such as the internal details of the engine, differentials, transfer case, etc. Essentially, three classes of non-rigid materials were used in the construction of the HMMWV:

(1) steel (of various grades);

(2) ballistic glass (used in windshields and windows); and

(3) rubber (used in tires).

The components of the transmission, suspension, and steering system were assumed to be made of AISI 4340 steel. The remaining components of the vehicle were taken to be made of one of the two mild steel grades with different initial yield strength levels.

A summary of the material models used in the present work to represent the structural and the ballistic response of the aforementioned materials is given in Table II, while a detailed account of these models can be found in Grujicic *et al.* (2008a). These models define the relationships between the flow variables (pressure, mass-density, energy-density, temperature, etc.) and involve:

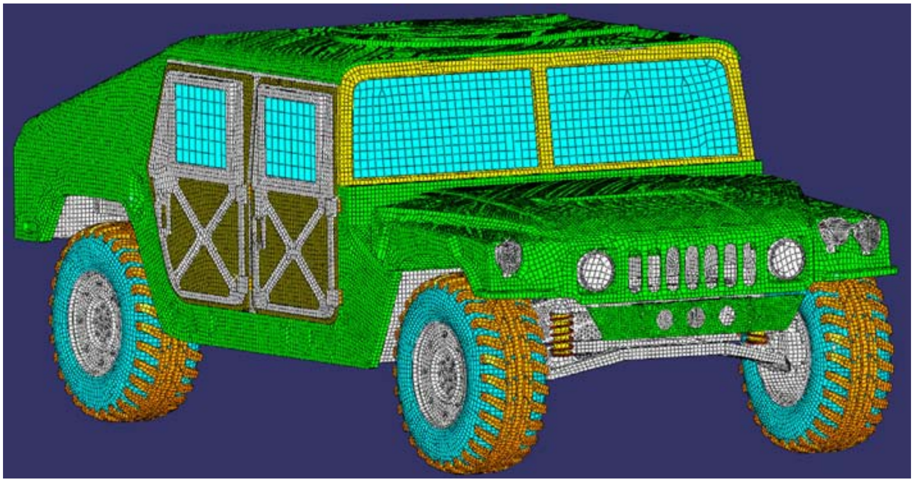

Figure 1. Geometrical meshed model for HMMWV vehicle used in the present work

Table II.
A summary of the material models used in the finite element of the off-road vehicle performance

Material	Equation of state	Strength	Failure	Erosion
Steel	Linear	Johnson-Cook (Johnson and Cook, 1983)	Johnson-Cook (Johnson and Cook, 1985)	Geometrical instantaneous strain
Rubber	Blatz-Ko hyper-elastic model (Blatz and Ko, 1962)		Maximum principal strain	Geometrical instantaneous strain
Glass	Linear	Linear-elastic	Hydro	Geometrical instantaneous strain
Sand	Compaction (Grujicic *et al.*, 2008a, b, 2009, 2010)	Compaction (Grujicic *et al.*, 2008a, b, 2009, 2010)	Hydro (Grujicic *et al.*, 2008a, b, 2009, 2010)	Geometrical instantaneous strain

- an equation of state;
- a strength equation;
- a failure equation; and
- an erosion equation for each constituent material.

These equations arise from the fact that, in general, the total stress tensor can be decomposed into a sum of a hydrostatic stress (pressure) tensor (which causes a change in the volume/density of the material) and a deviatoric stress tensor (which is responsible for the shape change of the material). An equation of state then is used to define the corresponding functional relationship between pressure, mass density and internal energy density (temperature). Likewise, a (constitutive material) strength relation is used to define the appropriate equivalent plastic strain, equivalent plastic strain rate, and temperature dependencies of the materials yield strength. This relation, in conjunction with the appropriate yield-criterion and flow-rule relations, is used to compute the deviatoric part of stress under elastic-plastic loading conditions. In addition, a material model generally includes a failure criterion (i.e. an equation describing the hydrostatic or deviatoric stress and/or strain condition(s) which, when attained, cause the material to fracture and lose its ability to support (abruptly in the case of brittle materials or gradually in the case of ductile materials) normal and shear stresses. Such failure criterion in combination with the corresponding material-property degradation and the flow-rule relations governs the evolution of stress during failure. The erosion equation is generally intended for eliminating numerical solution difficulties arising from highly distorted elements. Nevertheless, the erosion equation is often used to provide an additional material failure mechanism, especially in materials with limited ductility. To summarize, the equation of state along with the strength and failure equations (as well as with the equations governing the onset of plastic deformation and failure and the plasticity and failure induced material flow) enable assessment of the evolution of the complete stress tensor during a transient non-linear dynamics analysis. This assessment is needed where the governing (mass, momentum, and energy) conservation equations are being solved. Separate evaluations of the pressure and the deviatoric stress enable inclusion of the non-linear shock-effects in the equation of state (not important in the present work but highly critical when vehicle blast survivability is analyzed).

2.1.2 Geometrical modeling of the sand-bed region(s). Two sand-bed computational domains are used in the present work:

(1) a $L \times W \times H = 10{,}000 \times 2{,}800 \times 400$ mm, straight bed, Figure 2(a), used in the straight-line braking maneuvers; and

(2) a $L \times W \times H = 12{,}500 \times 2{,}800 \times 400$ mm, curved bed (radius of curvature equals to 4,300 mm and the angle subtended equals to 780), Figure 2(b), used in the sharp left-turn maneuvers.

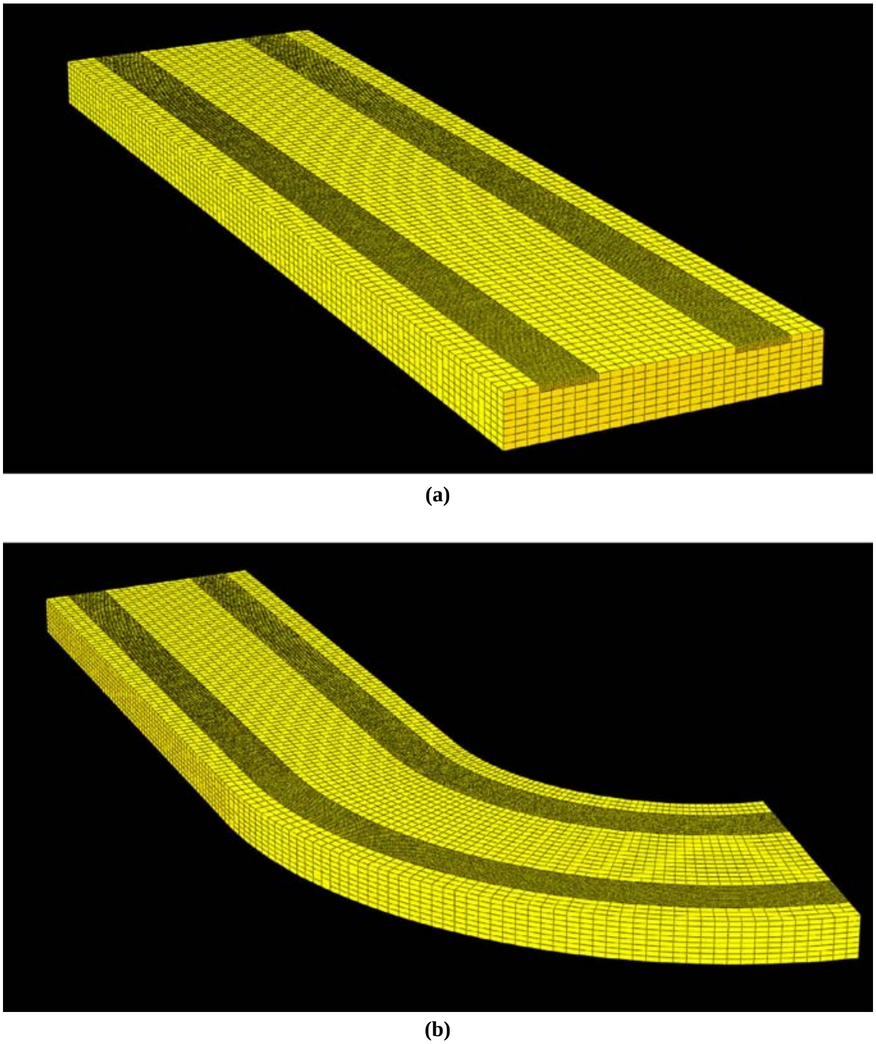

Notes: (a) Both straight-line braking maneuvers; (b) sharp left-turn maneuver

Figure 2.
Geometrical meshed models for sand-bed

Both sand-beds were meshed using solid eight-node reduced-integration elements with hourglass stiffening. Finer elements (ca. $10 \times 10 \times 10$ mm) were used in the "track" regions to more accurately quantify tire/sand interactions. To ensure seamless connection between the track sections and the rest of the sand-bed, surface-to-surface tie kinematic constraints were applied along the contacting surfaces of the finely and coarsely meshed sand-bed regions.

To model the constraining effects of sand surrounding the sand-bed, fixed boundary conditions were applied to the side and bottom faces of the sand-bed. A standard mesh-sensitivity analysis was carried out (the results not shown for brevity) in order to ensure that the results obtained are insensitive to the size of the elements used.

Sand is modeled using the CU-ARL sand model jointly developed by Clemson University and the Army Research Laboratory (ARL), Aberdeen, Proving Ground, MD (Grujicic *et al.*, 2006, 2009). For the CU-ARL sand model, a saturation-dependant porous-material/compaction equation of state is used within which separate pressure vs density relations are defined for plastic compaction (gives rise to the densification of sand) and for unloading/elastic-reloading. For the strength model, the shear modulus and the yield strength are assumed to be pressure dependant and to be controlled by saturation-dependant inter-particle friction. A "hydro" type failure model is adopted within which failure is assumed to occur when the negative pressure falls below a critical saturation-dependant value. Erosion of a sand element is assumed, within the CU-ARL sand erosion model, to take place when geometrical (i.e. elastic plus plastic plus damage) instantaneous strain reaches a maximum allowable value. A summary of the CU-ARL sand-model relations is given in Table II.

2.1.3 Modeling of the tire/sand interactions. The tire/sand interactions are modeled using the so-called "Hard contact pair" contact algorithm. Within this algorithm, contact pressures between two bodies (or between two sections of the same body) are not transmitted unless the nodes on the "slave surface" contact the "master surface". No penetration/over closure is allowed and there is no limit to the magnitude of the contact pressure that could be transmitted when the surfaces are in contact. Transmission of shear stresses across the contact interfaces is defined in terms of a static and a kinematic friction coefficient and an upper-bound shear stress limit (a maximum value of shear stress which can be transmitted before the contacting surfaces begin to slide).

2.1.4 Problem description. In this section, a brief description is provided of the transient non-linear dynamics computational finite-element analysis used in the present work to investigate the behavior of the two HMMWV configurations during straight-line braking and sharp left-turn off-road maneuvers.

Straight-line flatland braking. The straight-line flatland braking off-road maneuver was investigated using three loading steps:

(1) The vehicle is first lowered to the sand-bed and allowed to reach the state of static equilibrium (step duration 0.2 s).

(2) Next, the vehicle is accelerated over a time period of 0.8 s at a constant acceleration to a cruise velocity of 27 km/h. The velocity of the vehicle was controlled by prescribing a time-dependant velocity to the vehicle's center of gravity. During this step, the rotational velocity was prescribed to the wheels so that the pure rolling (i.e. the zero longitudinal-slip) condition is attained.

(3) The braking step is carried out by linearly decreasing with time the rotational velocity of all four wheels (the wheels' translational velocity boundary condition was removed).

Straight-line off-angle downhill braking. The same three aforementioned loading steps are used in the present section to study vehicle performance during a straight-line off-angle downhill braking maneuver. Instead of rotating the vehicle and road with respect to the global coordinate system while keeping the gravity direction along the z-axis, the gravity orientation was manipulated while the initial orientations of the vehicle/sand were retained. The gravity direction was rotated in two steps:

(1) First, the gravity vector was rotated about the global y-axis to account for the downhill-slope of the sand road.

(2) Then, the gravity vector was additionally rotated around the global z-axis to account for the angle between the direction of vehicle travel and the straight-downhill direction.

Sharp left-turn maneuver. The same first two steps are, again, applied as in the case of straight-line flatland braking. In the third step, which started at the end of the straight portion of the curved sand-bed; however, instead of braking, the vehicle was steered to the left. This was accomplished by applying time-dependant x- and y-translational velocities and a z-rotational velocity to the vehicle body, while properly steering the front wheels. The translational and rotational velocities were determined in such a way that, while maintaining the same translational (tangent) vehicle velocity of 27 km/h, the front-axle and rear-axle mid-points remained positioned above the sand-bed center-line. Front-wheel steering, on the other hand, was prescribed in such a way that the front wheels remained tangent to the sand-bed edges during the sharp left turn. An example of the time dependant x- and y-translational velocities and z-rotational velocity applied to the vehicle sprung mass and the additional z-rotational velocity applied to the front wheels is shown in Figure 3(a) and (b).

2.2 MBDs modeling of the off-road performance of an HMMWV

2.2.1 A MBDs model for HMMWV M1025. A new 36 degree of freedom MBDs model for HMMWV M1025 was developed in this work using various public-domain data. The model contains 40 rigid bodies and the addition of several force and control elements. A topological map of the HMMWV M1025 MBD model is shown in Figure 4. The basic kinematics of the model can be described as follows:

- The vehicle chassis, including cargo/load, is represented by a single rigid body.
- Eight rigid bodies are used to represent four lower A-arms and four upper A-arms. Each of the A-arms is connected to the chassis body by a single revolute joint with the axis of revolution initially aligned in the global x-direction.
- Four additional rigid bodies are used to represent the four wheel hubs each connected to a lower A-arm/upper A-arm pair. In the front of the vehicle, universal joints with their axes of revolution initially aligned in the global x- and z-direction are used for connection while, in the rear, revolute joints were used with their axis of revolution initially aligned in the global x-direction.

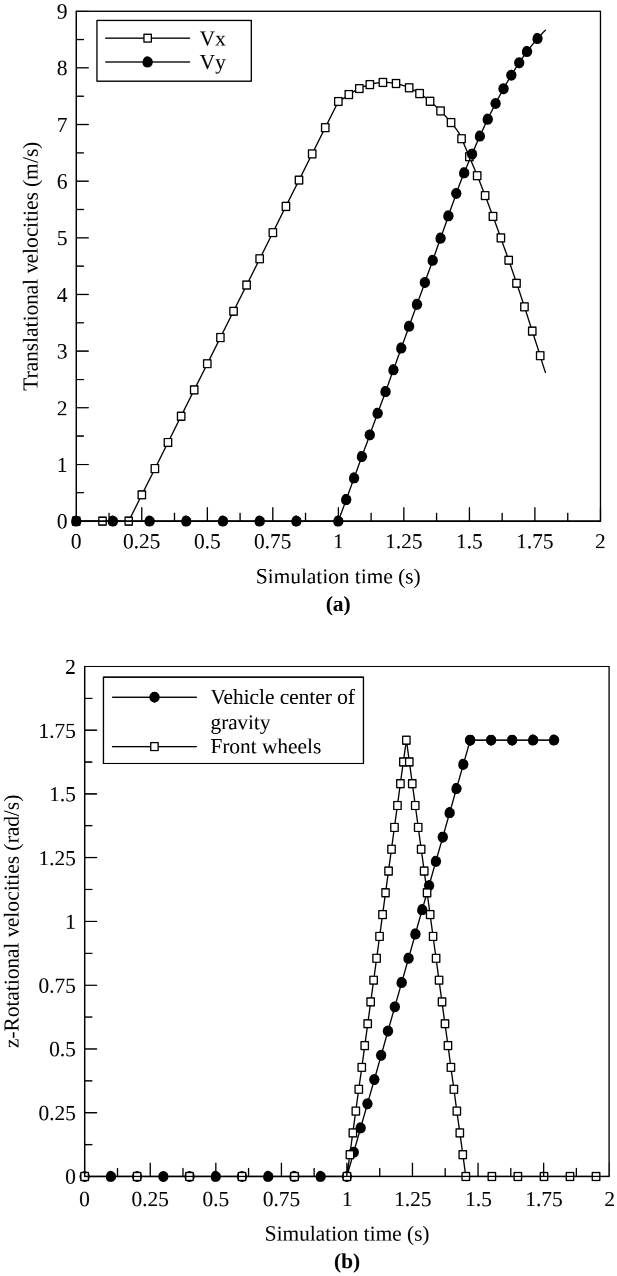

Figure 3.
Temporal evolution of the: (a) translational and (b) rotational velocities used as time-dependant boundary conditions applied at the vehicle/wheels during the sharp left-turn maneuver

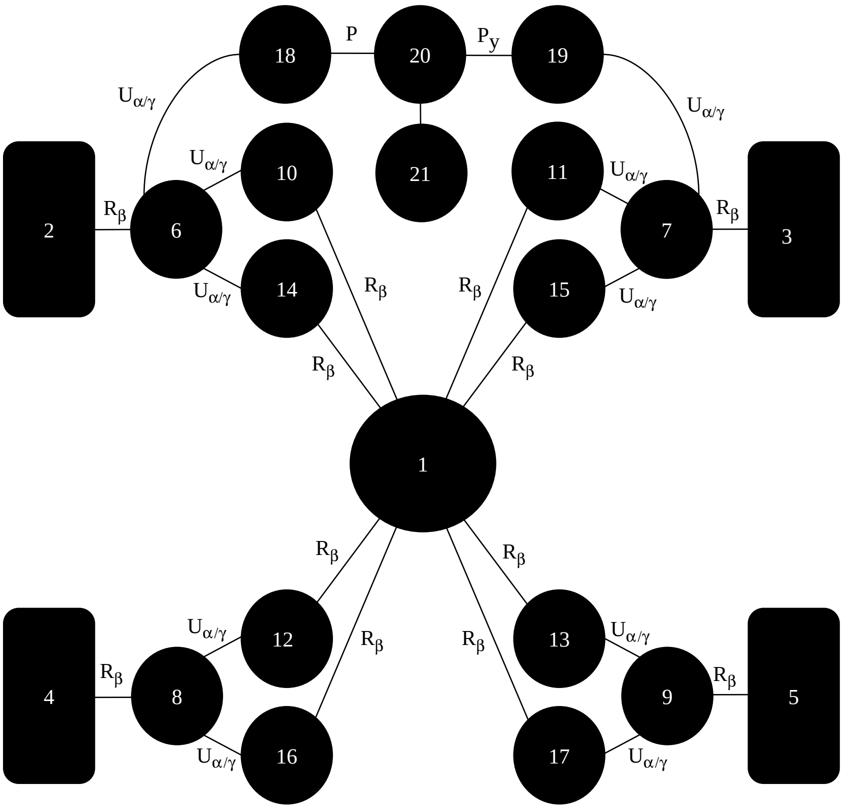

Notes: 1, Chassis; 2, FL wheel; 3, FR wheel; 4, RL wheel; 5, RR wheel; 6, FL wheel hub; 7, FR wheel hub; 8, RL wheel hub; 9, RR wheel hub; 10, FL upper A-arm; 11, FR upper A-arm; 12, RL upper A-arm; 13, RR upper A-arm; 14, FL lower A-arm; 15, FR lower A-arm; 16, RL lower A-arm; 17, RR lower A-arm; 18, steering rod L; 19, steering rod R; 20, steering rack; 21, steering column; R_β, revolute β joint; $U_{\alpha/\gamma}$, universal α/γ joint; P_y, translational y joint; TtF, torque-to-force; FL, front left; FR, front right; RL, rear left; RR, rear right; L, left; R, right

Figure 4. Topological map for the HMMWV M1025 MBDs model

- Four rigid bodies are used to represent the wheels which are connected to the wheel hubs using transverse revolute joints with their axis of revolution initially aligned in the global *y*-direction (i.e. along the wheels axis).
- Within the steering system, four rigid bodies are used to represent, respectively, the steering column, the steering rack and two steering rods. A single revolute joint is assigned to the steering column with its axis of revolution aligned with the axis of the column. A control element is used to provide input to this joint in order to enable controlled steering. Two prismatic joints with their translational axis initially aligned in global *y*-direction are used to connect the steering rack with the steering rods (one at each side of the vehicle). The steering rods were

connected to the wheel hub using universal joints which enable the revolutions other than the one along the axis of the steering rod. A "torque-to-force" constraint is placed between the steering column and the steering rack.

- Several hard and soft mechanical stops were used in order to adequately account for inter-component contacts. These stops were modeled as non-linear axial or rotational springs.
- Compliance of the suspension system was represented by connecting axial springs and shock absorbers between the upper shock-mount of the chassis and the lower shock-mount located on the lower A-arm and the appropriate spring rates and damping coefficients were assigned.
- The vertical force developed between the standard tire used on an HMMWV and a rigid-ground surface as a function of the vertical tire-deflection was taken from tests performed on this tire and includes "bottoming-out" hardening effects (Shoop, 2001).
- The non-linear longitudinal friction/shear behavior of the tire on a rigid road was modeled using the Pacejka (1966) magic formula and the tire/road interaction forces are set to zero when the tire is not in contact with the ground. The longitudinal force is a function of the relative velocities between the bottom of the tire and the ground (i.e. the longitudinal slip), the normal force and the tire/road friction coefficient. Similarly, the lateral shear force is calculated using the slip angle (obtained using the forward and lateral slip velocity components), friction coefficient and the vertical force.
- The behavior of the same tire on a deformable sand-based road is discussed in next section.

A MBDs model like the one developed in the present work requires the knowledge of initial position and orientation of every component and any interconnecting joints as well as individual component mass/inertia properties. This yields a very detailed model of the suspension and steering including elements such as upper and lower A-arms, steering link and tie rods.

2.2.2 MBDs off-road vehicle performance calculations. All calculations carried out in this portion of the work were done using Simpack (Intec, 2008) is a highly detailed general-purpose transient non-linear-dynamics modeling and simulation computer program capable of analyzing the response of controlled, articulated multi-body mechanical systems when subjected to various (regular or irregular) external and internal effects. The program contains an extensive library of primitive rigid (and flexible) bodies, kinematic joints, and force and controlled elements which can be combined in various ways in order to assemble complex-system models at a level of details considered necessary in the problem at hand. Simpack comprises three main modules:

(1) a pre-processor;

(2) a main processor; and

(3) a post-processor.

Within the pre-processor, topological, and parametric properties of the model are defined within an interactive environment. The processor uses the information defined by the pre-processor to assemble the governing kinematics and dynamics equations. In addition, the processor may take advantage of one or more user-interface subroutines which allow the incorporation of highly non-linear vehicle-system properties and, thus, can yield quite representative/realistic models. Finally, the processor carries out numerical integration of the governing equations of motion for a specified time period, and, outputs computed values of the system states at regular time intervals. Within the post-processor, these results could be displayed as time traces or cross-plotted, or combined with the geometrical entities of the model to produce animations.

The same three off-road vehicle maneuvers are analyzed as in the case of the finite element analysis. To steer and break the vehicle, appropriate time excitations were applied to different system degrees of freedom. The (straight and curved) flatland and downhill conditions of the sandy road were constructed using the "track" and "road" utilities of SIMPACK (Intec, 2008).

2.2.3 Tire/sand interaction model. Owing to normal-sinkage and forward/sideways ploughing effects of the wheels in sand, and the accompanying motion resistance, an off-road computational dynamics analysis, of the wheeled vehicles is quite a bit more complicated than the corresponding analysis dealing with the same vehicle travelling on a hard-surface road (an on-road analysis) (Wong, 1989). To account for the aforementioned off-road vehicle travel effects, the tire/rigid-road model mentioned in the previous section had to be abandoned and replaced with a tire/sandy-road model.

The tire/sandy-road model used was the one recently developed by Grujicic *et al.* (2010) by carrying out a series of transient, non-linear dynamics finite element analyses of the interactions between the Goodyear Wrangler HT 235/75 R15 and sand during off-road vehicle travel. The interactions were considered under different combined conditions of the longitudinal and lateral slip as encountered during "brake-and-turn" and "drive-and turn" vehicle maneuvers. Different components of the pneumatic tire were modeled using elastic, hyper- and visco-elastic material models (with rebar reinforcements) while sand is modeled using the CU-ARL sand models (Grujicic *et al.*, 2006, 2009). The analyses were used to obtain functional relations between the wheel vertical load, wheel sinkage, tire deflection (gross) traction, motion resistance and the (net) drawbar pull. These relations were finally cast as a tire/sand non-linear force-element model suitable for use in MBDs computer programs. The basic constitutive relations defining the force elements include:

- the vertical force vs sinkage vs sinkage rate;
- the longitudinal traction force vs longitudinal slip vs normal force;
- the transverse force vs slip angle vs normal force; and
- the self-aligning moment vs slip angle vs normal force.

The tire/sand non-linear force-element model (Grujicic *et al.*, 2010) was implemented as a "utyre_spck.f" user tire-model subroutine in Simpack (Intec, 2008). Within this subroutine, the current values of the wheel-center kinematic parameters (e.g. vertical displacement, longitudinal displacement, rotational speed around the wheel axis, etc.) are used to calculate sinkage, sinkage rate, longitudinal slip and slip angle and, in turn, through the use of the force-element constitutive relations the normal and tangential forces and the associated moments/torques.

3. Results and discussion

In this section, the main results obtained in the present work pertaining to the effect of HMMWV up-armoring on the off-road vehicle performance are presented and discussed. As mentioned earlier, three off-road vehicle maneuvers were considered:

(1) straight-line flatland braking;

(2) straight-line off-angle downhill braking; and

(3) a sharp left-turn.

Hence, the results pertaining to the three maneuvers are presented first in the next three sections. Then, in Section 3.4, a brief discussion is presented regarding the overall effect of up-armoring on the off-road vehicle performance.

3.1 Straight-line flatland braking performance

An example of typical results pertaining to the HMMWV and sand-bed kinematics and deformation during straight-line flatland braking are shown in Figure 5(a) and (b). While both figures correspond to the condition of the maximum pitch angle/front-wheel sinkage, Figure 5(a) is obtained using the finite element analysis while Figure 5(b) is obtained using the MBDs calculations. Clearly, the results displayed in these figures are quite comparable (at least qualitatively).

When analyzing off-road straight-line flatland vehicle braking, the following performance criteria are generally considered:

(1) ability of the vehicle to regain traction following a hard braking maneuver to full stop;

(2) the ability of the vehicle to come to a full stop over a reasonably short braking distance; and

(3) the ability of the vehicle to come to a full stop without experiencing excessive pitching.

The three criteria described above were introduced in order of their perceived importance. It is well-established that a single phenomenon, the extent of front-wheel sinkage, affects all three aforementioned performance criteria and controls the tradeoffs between them. For example, deeper front wheel sinkage results in a shorter braking distance, but in turn increases the tendency for excessive pitching and may result in total loss of vehicle mobility ("may cause the vehicle to become stuck").

The effect of the average braking torque on the flatland braking distance for the standard configuration and the up-armored configuration of the HMMWV (at a 27 km/h vehicle velocity before the onset of braking) is shown in Figure 6(a). Both the finite element and the MBDs results are displayed in this figure. The results shown in Figure 6(a) reveal that:

- with increased braking torque (severity of braking) the vehicle braking distance is decreased;
- up-armoring compromises the HMMWV's straight-line flatland braking performance, i.e. to attain the same braking distance, a ~30-35 percent increase in the braking torque is required in the case of the up-armored vehicle; and

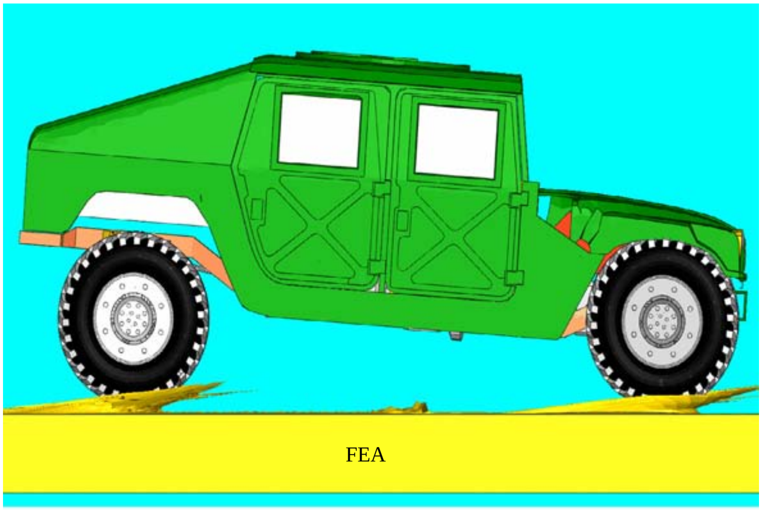

(a)

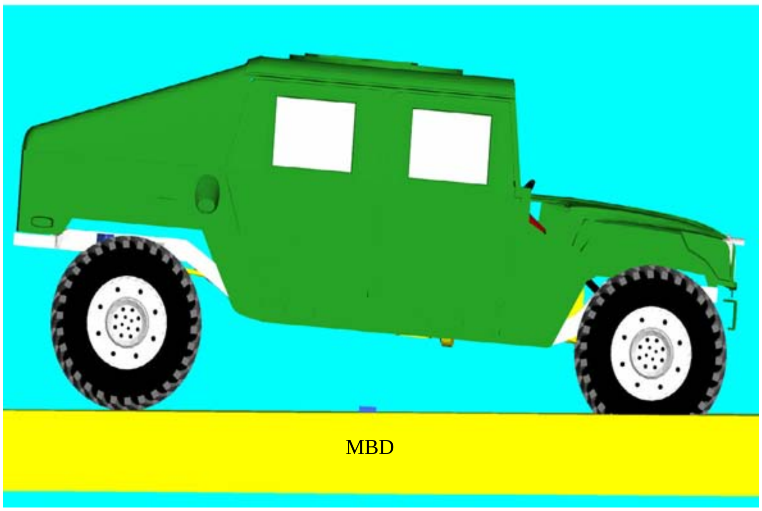

(b)

Notes: (a) Finite element analysis; (b) MBDs calculations

Figure 5.
Maximum pitch-angle HMMWV and sand-bed kinematics and deformation resulting from a straight-line flatland braking maneuver

- the finite-element and the MBDs results are in reasonably good agreement (i.e. the_ relative difference between the two sets of results is about 15 percent).

The effect of the average braking torque on the propensity for excessive vehicle pitching during a straight-line flatland braking maneuver for the standard configuration and the up-armored configuration of the HMMWV (at a 27 km/h vehicle velocity before the onset of braking) is shown in Figure 6(b). As expected, the results shown in Figure 6(b) show that both the severity of braking (quantified by the average braking torque) and

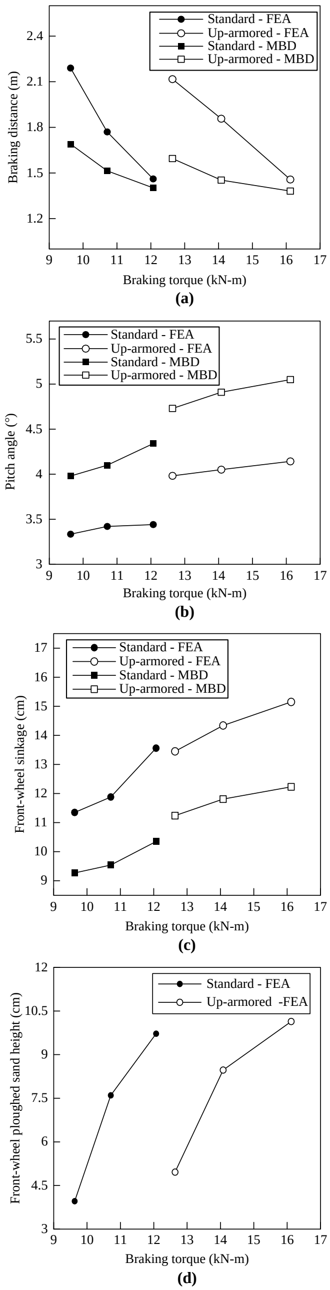

Notes: The pre-braking vehicle velocity = 27 km/h; FEA, the finite-element analysis results; MBD, the MBDs calculation results

Figure 6.
The effect of HMMWV up-armoring and the average braking torque on the: (a) braking distance; (b) pitch angle; (c) front-wheel sinkage; and (d) maximum height of the front-wheel ploughed sand, for the straight-line flatland braking case

up-armoring increase the pitch angle of the vehicle. While the overall range (3-4°) of the pitch angle is relatively small, up-armoring is seen to increase this angle by 20-25 percent. Again, the finite-element and the MBDs results are in reasonably good agreement.

The effect of the average braking torque on the maximum front-wheel sinkage for the standard configuration and the up-armored configuration of the HMMWV (at a 27 km/h vehicle velocity before the onset of braking) is shown in Figure 6(c). The results displayed in this figure reveal that both increased severity of braking and vehicle up-armoring result in an increase of the front-wheel sinkage. Reasonably, good agreement is once more seen between the finite-element and the MBDs results. A‘ comparison of the results shown in Figure 6(a)-(c) confirms that front-wheel sinkage indeed controls the vehicle performance during straight-line flatland braking.

The effect of the average braking torque on the extent of ploughed-sand buildup ahead of the front wheels during a straight-line flatland braking maneuver for the standard configuration and the up-armored configuration of the HMMWV (at a 27 km/h vehicle velocity before the onset of braking) is shown in Figure 6(d). As expected, the results shown in Figure 6(d) that both the severity of braking (quantified by the average braking torque) and up-armoring increase the height of the front-wheel ploughed-sand. It is critical to understand that the front-wheel ploughed sand buildup increases the effective front-wheel sinkage and may affect the vehicles ability to regain traction after braking to full-stop. Also, it should be noted that only the finite-element results are shown in Figure 6(d) since the corresponding results could not be generated using the MBDs calculations (i.e. in the MBDs analyses sand is modeled only implicitly through its interactions with the vehicle tires).

To examine the ability of the vehicle to regain traction after braking to a full stop, a constant rotational acceleration in a range between 1 and 32 rad/s^2 is applied to all four wheels of the vehicle while the forward motion and wheel sinkage of the vehicle are monitored.

The effect of restart angular wheel acceleration on the ability of the vehicle to regain traction following a straight-line flatland braking maneuver to full stop for the standard configuration and the up-armored configuration of the HMMWV is shown in Figure 7. In this figure, the ability of the vehicle to regain traction is quantified by a ratio of the forward motion of the vehicle over the additional front-wheel sinkage at the end of a 0.5 s acceleration period. Smaller values of this ratio correspond to the condition when a vehicle is more likely to become immobile due to further front-wheel sinkage (caused by the "shoveling"-action of the tire treads under large values of longitudinal slip and/or increased vehicle weight). The results shown in Figure 7 reveal that:

- For both the standard and the up-armored configurations there is an optimal value of the restart wheel angular acceleration at which the vehicle is most likely to regain traction (i.e. at which the ratio of the forward motion of the vehicle over the additional front-wheel sinkage is maximal).
- At lower restart angular accelerations, the visco-plastic behavior of the sand appear to have a dominant effect making the sand softer and causing an increase in vehicle sinkage.
- At larger restart accelerations, the sand "shoveling"-action of the tire treads appears to dominate also causing more pronounced vehicle sinkage.

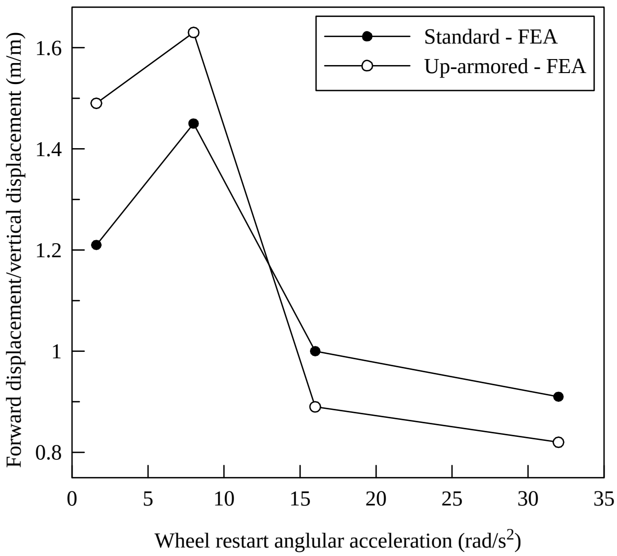

Note: The vehicle pre-braking velocity = 27 km/h

Figure 7.
The effect of HMMWV up-armoring on the vehicle's ability to regain traction after straight-line flatland braking under different wheel restart angular accelerations

- At lower restart accelerations, the up-armored configuration of the vehicle shows a superior restart performance. This effect appears to be associated with more pronounced strain hardening of the compacted sand underneath the vehicle tires giving rise to a lower vehicle sinkage in the up-armored configuration case.
- At higher restart accelerations, however, the restart performance of the up-armored vehicle is clearly inferior to that of the standard configuration.

3.2 Straight-line off-angle downhill braking performance
When analyzing straight-line off-angle downhill vehicle braking, the main performance criterion generally considered is the loss of vehicle stability. This instability is manifested in the following three ways:

(1) rear-to-front wheel load-transfer induced pitching which may cause the rear wheels to loose contact with the ground;
(2) yaw-rotation of the vehicle about the downward-most front wheel (the wheel whose center has the lowest altitude); and
(3) vehicle roll towards the downhill direction.

The effect of up-armoring on the vehicle tendency to become unstable during a straight-line off-angle downhill braking maneuver is shown qualitatively in Figure 8(a)-(d), the finite-element results, and Figure 9(a)-(d), the MBDs results. The results displayed in these figures pertain to the case of a straight-line off-angle 30° downhill braking where the angle between the vehicle-travel direction and the straight-downhill direction (i.e. the downhill lateral-travel direction) is 45°. In Figures 8 and 9, parts (a) and (c) pertain to the standard vehicle configuration, while parts (b) and (d) pertain to the up-armored configuration. Also, parts (a) and (b) show top-views

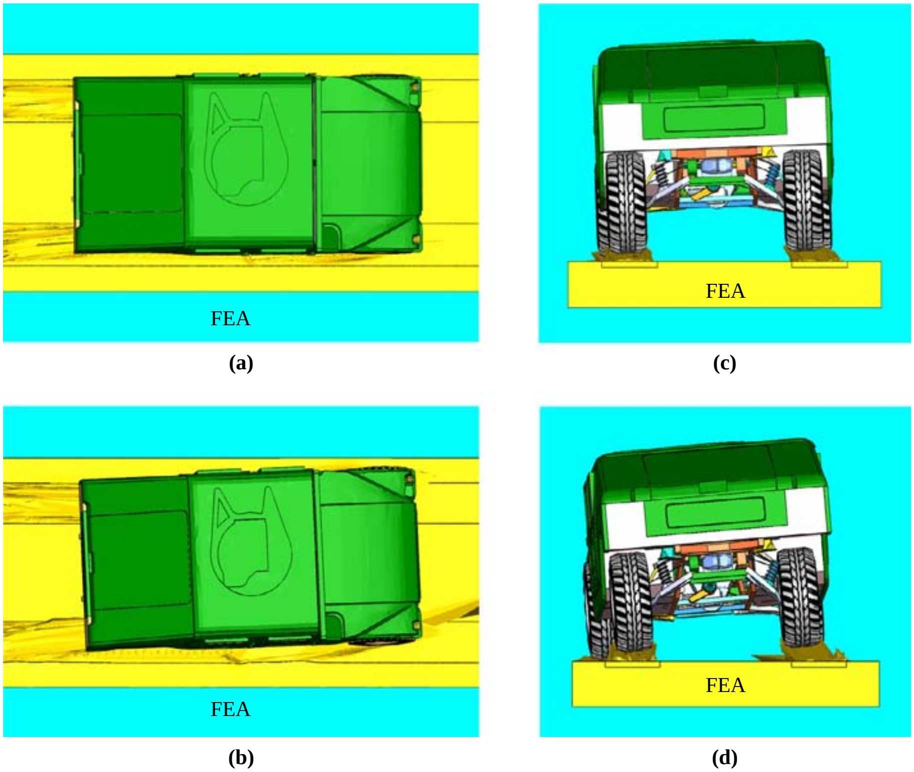

Notes: (a) and (c) Standard vehicle configuration; (b) and (d) up-armored configuration; (a) and (b) top views; and (c) and (d) rear views; pre-braking velocity = 27 km/h; please see text for details

Figure 8. Qualitative evidence for the up-armoring increased rollover propensity in the HMMWV during a downhill braking maneuver obtained using finite-element analysis

(i.e. the view along the global negative z-axis), while parts (c) and (d) depict rear-views (i.e. the view along the global positive x-axis). The pre-braking velocity was 27 km/h. A comparison of the corresponding parts of Figures 8(a)-(d) and 9(a)-(d) show a reasonable agreement between the results obtained using the finite-element analysis and the MBDs calculations.

3.3 Sharp-turn performance

Temporal evolution of the HMMWV and sand-bed during a typical sharp left turn is shown in Figure 10(a)-(d), the finite-element results, and Figure 11(a)-(d), the MBDs results. The lift-off of the inside wheels, increased sinkage of the outside wheels due to the inside-to-outside wheel weight transfer and the resulting vehicle roll-over are clearly seen in these figures.

When analyzing off-road sharp-turn behavior, the main vehicle performance criterion is the propensity to rollover. As in the case of off-road straight-line flatland braking, the dominant phenomenon controlling vehicle stability with respect to rollover is the extent of outside-wheel sinkage and the associated plowing-induced sand buildup. That is, deeper outside-wheel sinkage and greater sand buildup promote vehicle rollover during sharp-turn maneuvers. This effect can be rationalized as

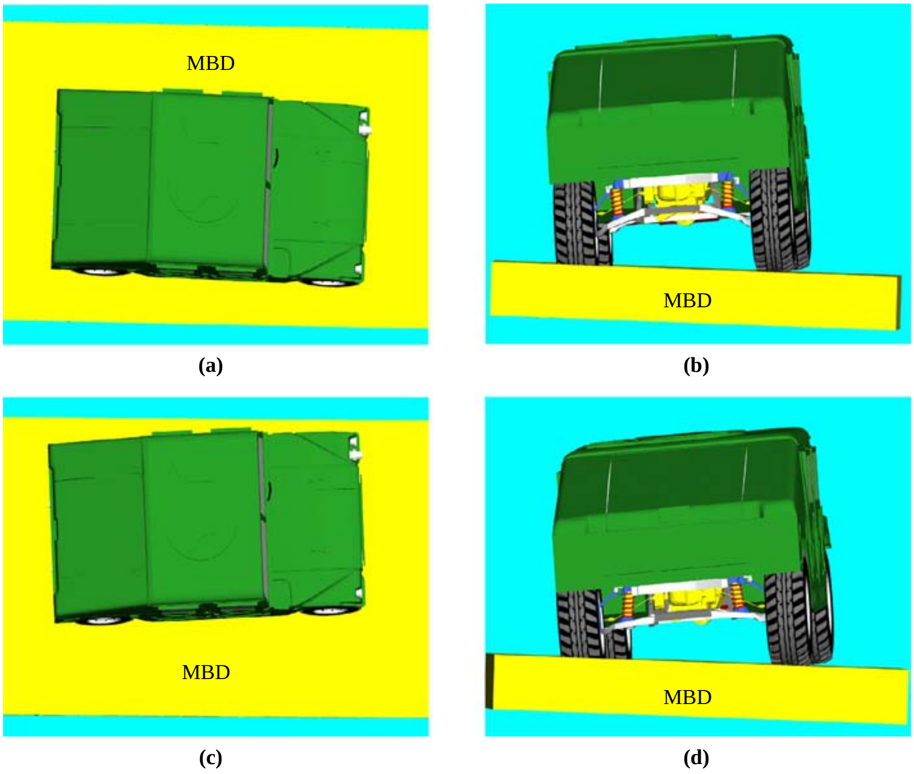

Figure 9.
Qualitative evidence for the up-armoring increased rollover propensity in the HMMWV during a downhill braking maneuver obtained using MBDs analysis

Notes: (a) and (c) Standard vehicle configuration; (b) and (d) up-armored configuration; (a) and (b) top views; and (c) and (d) rear views; pre-braking velocity = 27 km/h; please see text for details

follows: the outside-wheel sinkage causes the weight of the vehicle to act at a position that is laterally offset with respect to the track center leading to a decrease in the stabilizing (anti-rollover) moment. In addition, the wheel-sinkage and sand buildup increase the lateral reaction force acting on the outside wheels. This reaction force in combination with the lateral acceleration force forms a couple, i.e. a destabilizing (rollover) moment.

The effect of lateral acceleration and vehicle up-armoring on the minimum vertical force acting on the inside wheels of the vehicle during a sharp-turn maneuver is shown in Figure 12. The results displayed in this figure can be used to quantify the vehicle's propensity to rollover. This propensity is defined as the lowest lateral acceleration at which the vertical force acting on the inside wheels of the vehicle attains a zero value. Clearly, the results shown in Figure 12 show that up-armoring causes the vehicle to become more susceptible to rollover during sharp-turn maneuvers. In the present case, up-armoring is found to increase rollover propensity (i.e. decreases the critical lateral acceleration at which the inside-wheel vertical force becomes zero) by 10-15 percent.

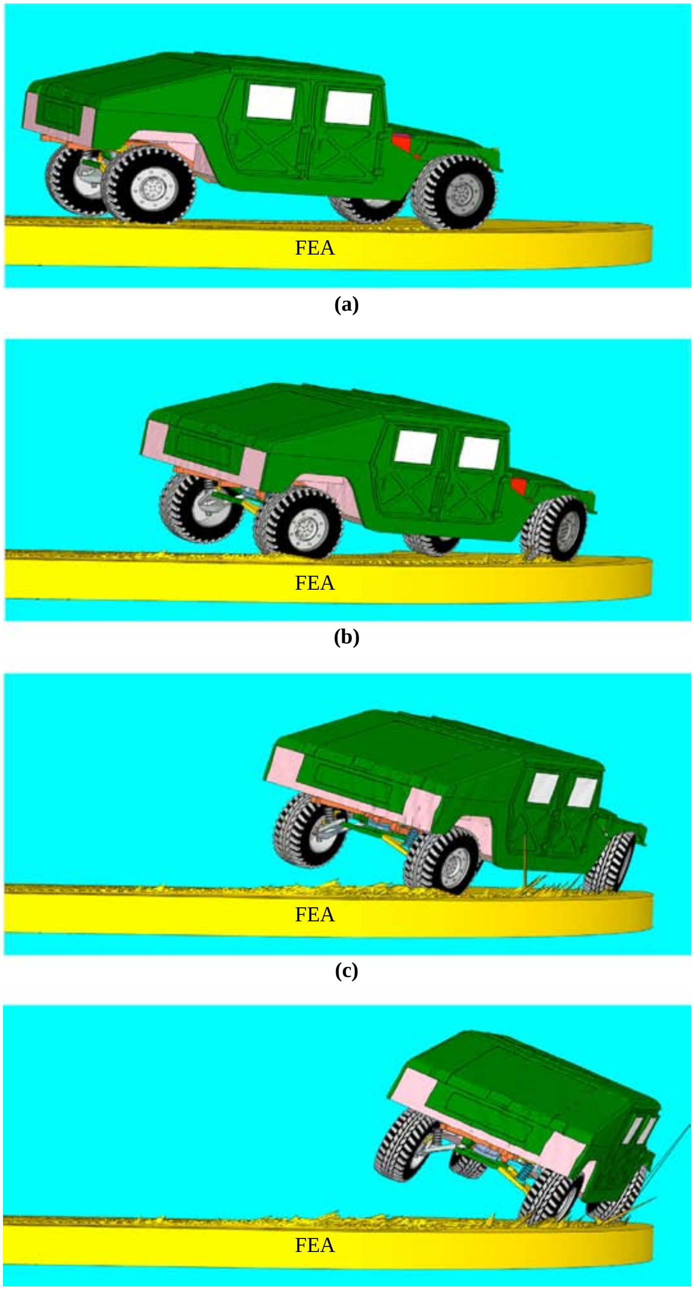

Note: The finite-element analysis results

Figure 10.
Temporal evolution of the HMMWV and the sand-bed kinematics and deformation during a sharp left-turn maneuver

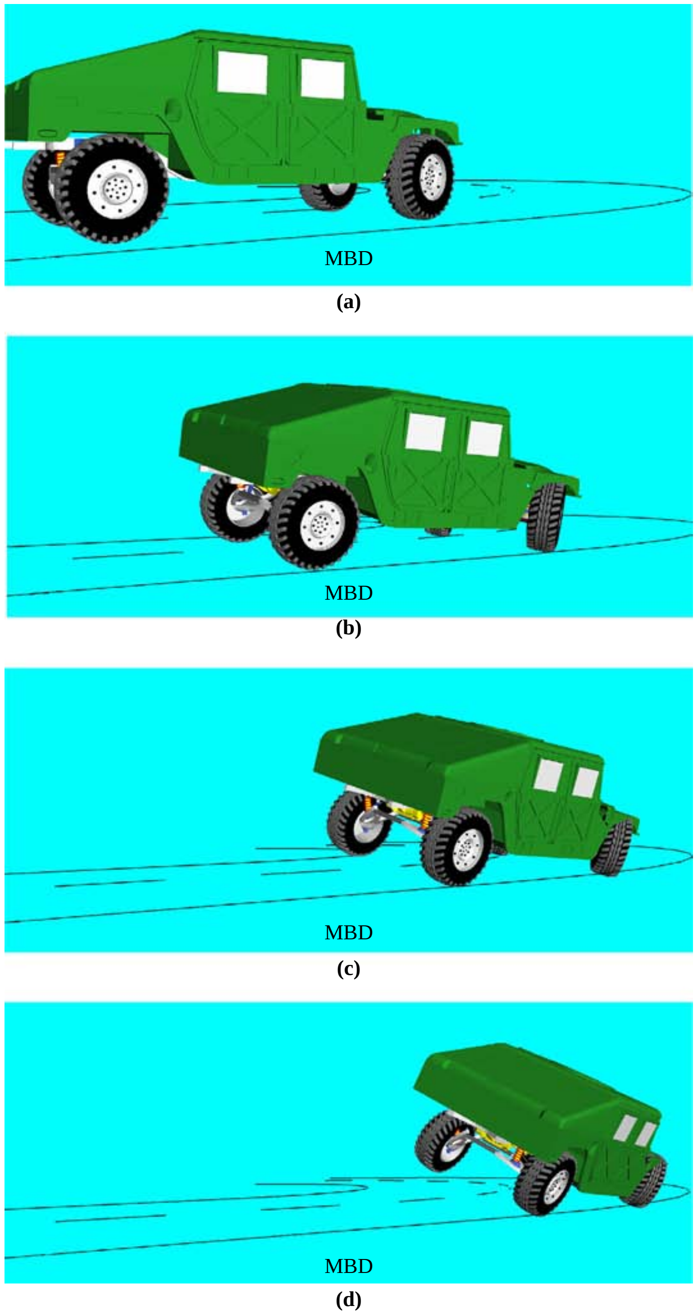

Note: The MBDs calculation results

Figure 11.
Temporal evolution of the HMMWV and the sand-bed kinematics and deformation during a sharp left-turn maneuver

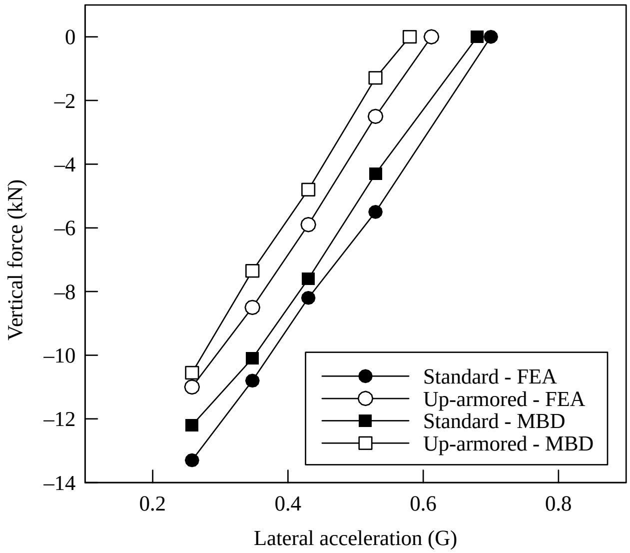

Notes: The pre-turn velocity = 27km/h; FEA, the finite-element analysis results; MBD, the MBDs calculation results

Figure 12.
The effect of lateral acceleration and HMMWV up-armoring on the vehicle propensity to undergo rollover during a sharp left-turn maneuver

3.4 A brief discussion regarding the effect of up-armoring

The computational investigation carried out in the present work clearly revealed that up-armoring of light tactical military vehicles, like the HMMWV, can have serious negative consequences on the off-road performance and stability of these vehicles. Specifically, the present investigation revealed that:

- During flatland braking, up-armored vehicles tend to require longer braking distances, and experience greater pitch angles and front-wheel sinkage. The latter two effects may, in turn, lead to lesser ability of the vehicle to regain traction after coming to a full stop. In addition, greater wheel-sinkage is typically associated with higher values of the longitudinal motion resistance. This increase can be attributed to a larger volume of the sand which has to be compacted during vehicle forward travel. Greater motion resistance gives rise to larger forces experienced by the suspension and drive-train and inevitably leads to a shorter service life of these components.
- During straight-line off-angle downhill braking up-armored vehicles clearly showed higher propensity to instability and loss of control. This instability can lead to vehicle rollover and may result in occupants injuries and fatalities.
- Similar instabilities and increased tendencies to vehicle rollover are observed in up-armored vehicles during sharp turns. These effects can be attributed to greater sinkage experienced by the outside wheels. Furthermore, as in the case of the flatland braking, increased wheel sinkage may result in larger motion resistance; however, in this case it is the lateral motion resistance which is increased. The mechanism controlling this increased motion resistance is the larger volume of sand that has to be ploughed laterally.

To overcome some of the aforementioned up-armoring induced deficiencies in the off-road vehicle performance while maintaining its blast/ballistic protection performance and survivability, different design/manufacturing approaches could be employed, such as:

- various light-weight engineering concepts can be utilized;
- future vehicles could be designed with variable ride-height suspension (to lower the center of gravity) and a larger track width; and
- improved tire engineering could be used to reduce the extent of wheel sinkage while maintaining traction.

In our ongoing work, the several light-weight engineering strategies are being analyzed in order to better understand their full potential. The outcome of this investigation will be reported in our future communications.

It should be recalled that one of the objectives of the present work was to examine the ability of a computationally efficient MBDs approach when combined with a detailed model for tire/soil interactions to yield results qualitatively and quantitatively consistent with their computational counterparts obtained using computationally quite costly finite element analyses. Typically, the MBDs analyses were 15-20 times faster their finite-element counterparts. The results obtained in the present work suggest that relatively good agreement (i.e. relative difference is $<$ ca. 20 percent) between the two approaches is possible. As correctly pointed out by one of the reviewers of the present work, the reason for the observed differences in the finite element analysis and MBDs based off-road performances of the vehicle could be the result of the fact that the vehicle chassis was modeled as a single-rigid body. Per reviewers' suggestion, a preliminary investigation was conducted in which the deformability of the chassis within the MBDs framework was accounted for through the use of a reduced-order model generated from the full-order finite element analysis model. This investigation revealed that while some improvements in the agreement between the two sets of results is attained, significant differences remained.

The present work also revealed that for some aspect of the vehicle off-road performance (e.g. the ability of the vehicle to regain traction after coming to a full stop) which entails the knowledge of ploughed/bulldozed sand height, the use of finite element calculations is still required. In the case of the finite-element analysis, ploughed/bulldozed sand height is obtained as one of the results of the straight-line braking analysis. On the other hand, when MBDs is used to simulate straight line braking, this quantity cannot be determined. Consequently, when MBDs is used to model restarting of the vehicle, one must provide, as input, the value of the ploughed/bulldozed sand height.

4. Summary and conclusions

Based on the results obtained in the present work, the following main summary remarks and conclusions can be drawn:

- A comprehensive parallel finite-element/MBDs investigation of the off-road performance of a prototypical HMMWV in a standard and up-armored configuration is carried out.
- The first vehicle off-road maneuver investigated, i.e. straight-line flatland braking, clearly revealed the negative effect of up-armoring on the braking

distance, on the vehicle propensity for excessive pitching, and the ability of the vehicle to regain traction upon coming to a full stop.

- The second vehicle off-road maneuver investigated, i.e. straight-line off-angle downhill braking, provided qualitative evidence of increased vehicle instability and potential for rollover (the condition which generally leads to vehicle-occupants injuries/fatalities) resulting from vehicle up-armoring.
- Within the final vehicle off-road maneuver investigated, i.e. a sharp left-turn, vehicle up-armoring was also found to lead to a higher rollover propensity.
- In general, the highly efficient MBDs calculations based on the use of high-fidelity tire/soil interaction models are capable of producing off-road vehicle-performance results comparable to their counterparts obtained using more-costly finite-element calculations. However, for some aspect of this performance the use of finite-element calculations is still required.

References

Altair Engineering (2010), *Hypermesh Version 10.0*, Altair, Auckland, available at: www.altair.com

Blatz, P.J. and Ko, W.L. (1962), "Application of finite elasticity to the deformation of elastic materials", *Transactions of the Society of Rheology*, Vol. 6, pp. 227-51.

CAD Browser (2010), available at: www.3dcadbrowser.com/preview.aspx?ModelCode=12399

Dassault Systems (2008), *ABAQUS Version 6.8-1, User Documentation*, Dassault Systems, Paris.

Grujicic, M., Pandurangan, B. and Cheeseman, B.A. (2006), "The effect of degree of saturation of sand on detonation phenomena associated with shallow-buried and ground-laid mines", *Shock and Vibration*, Vol. 13, pp. 41-61.

Grujicic, M., Arakere, G., Bell, W.C. and Haque, I. (2009), "Computational investigation of the effect of up-armoring on occupant injury/fatality reduction of a prototypical high-mobility multi-purpose wheeled vehicle subjected to mine-blast", *Journal of Automobile Engineering*, Vol. 223, pp. 903-20.

Grujicic, M., Bell, W.C., Arakere, G. and Haque, I. (2008a), "Finite element analysis of the effect of up-armoring on the off-road braking and sharp-turn performance of a high-mobility multi-purpose wheeled vehicle (HMMWV)", *Journal of Automobile Engineering*, Vol. 223, D11, pp. 1419-34.

Grujicic, M., Marvi, H., Arakere, G. and Haque, I. (2010), "A finite element analysis of pneumatic-tire/sand interactions during off-road vehicle travel", *Multidiscipline Modeling in Materials and Structures* Vol. 6 No. 2, pp. 284-308.

Grujicic, M., Pandurangan, B., Haque, I., Cheeseman, B.A., Roy, W.N. and Skaggs, R.R. (2007), "Computational analysis of mine blast on a commercial vehicle structure", *Multidiscipline Modeling in Materials and Structures*, Vol. 3, pp. 431-60.

Grujicic, M., Pandurangan, B., Cheeseman, B.A., Roy, W.N., Skaggs, R.R. and Gupta, R. (2008b), "Parameterization of the porous-material model for sand with various degrees of water saturation", *Soil Dynamics and Earthquake Engineering*, Vol. 28, pp. 20-35.

Hahn, Y., Hulbert, G., Ma, Z., Liu, Q. and Lee, J. (2007), "Off-road vehicle dynamic simulation based on slip-shifted on-road tire handling model", SAE Technical Paper 08MV-5, SAE International, Warrendale, PA.

Intec (2008), *SIMPACK Version 8900, User Documentation*, Intec, Indianapolis, IN.

Johnson, G.R. and Cook, W.H. (1983), "A constitutive model and data for metals subjected to large strains, high strain rates and high temperatures", *Proceedings of the 7th International Symposium on Ballistics, The Hague, The Netherlands*.

Johnson, G.R. and Cook, W.H. (1985), "Fracture characteristics of three metals subjected to various strains, strain rates and temperatures", *Engineering Fracture Mechanics*, Vol. 21 No. 1, pp. 31-48.

Law, E.H., Tremblay, J.E., Bergeron, D.M. and Gonzalez, R. (1998), "Protection of soft-skinned vehicle occupants from landmine blasts", The Technical Cooperation Program, Subcommittee on Conventional Weapons Technology, Technical Panel W-1, Key Technical Activity 1-29, Sydney.

Lee, J. and Kiu, Q. (2007), "Modeling and simulation of in-plane and out-of-plane forces of pneumatic tires on fresh snow based on the finite element method", *Proceedings of the Joint North America, Asia-Pacific ISTVS Conference and Annual Meeting of Japanese Society for Terramechanics, University of Alaska, Fairbanks, AK, USA*.

Pacejka, H.B. (1966), "The wheel shimmy phenomenom: a theoretical and experimental investigation with particular reference to the nonlinear problem (analysis of shimmy in pneumatic tires due to lateral flexibility for stationary and nonstationary conditions)", PhD thesis, Delft University of Technology, Delft.

Shoop, S.A. (2001), "Finite element modeling of tire-terrain interaction", CRREL Technical Report, ERDC/CRREL TR-01-16, US Army Cold Regions Research and Engineering Laboratory, Hanover, NH.

Stewart, J. (2006), "Investigation of rollover, ride, lateral handling and obstacle avoidance maneuvers of tactical vehicles", Clemson University Department of Mechanical Engineering Report TR-06-106-ME-MMS, Clemson University, Clemson, SC.

Wong, J.Y. (1989), *Terramechanics and Off-road Vehicles*, Elsevier, Amsterdam.

About the authors

M. Grujicic is a Professor of Materials Engineering in Clemson University. His research interests include computational engineering. M. Grujicic is the corresponding author and can be contacted at: mica.grujicic@ces.clemson.edu

H. Marvi is a PhD student in Clemson University. He specializes in engineering dynamics.

G. Arakere is a PhD student in Clemson University. His research interests include computational modeling.

W.C. Bell is a PhD student in Clemson University. His research interests include computational modeling.

I. Haque is a Professor of Mechanical and Automotive Engineering in Clemson University. He specializes in the area of vehicle dynamics.